A conservative all Mach number semi-implicit finite volume method for magnetically-dominated visco-resistive MHD

A. Farmakalides, R. Dematte, N.Nikiforakis, S. Millmore
Centre for Scientific Computing, University of Cambridge

Introduction

- The VRMHD system of equations can be solved to simulate disruption events in tokamaks such as ELMs and VDEs.

$$\frac{\partial}{\partial t}\begin{bmatrix}\rho\\ \rho\mathbf{v}\\ \rho E\\ \mathbf{B}\end{bmatrix}+\nabla\cdot\begin{bmatrix}\rho\mathbf{v}\\ \rho\mathbf{v}\otimes\mathbf{v}+p_{mag}\mathbf{I}-\mathbf{B}\otimes\mathbf{B}\\ \mathbf{v}^T(\rho E+p_{mag})-\mathbf{v}^T\mathbf{B}\otimes\mathbf{B}\\ \mathbf{B}\otimes\mathbf{v}-\mathbf{v}\otimes\mathbf{B}\end{bmatrix}=\nabla\cdot\mathbf{F}^{VR}$$

where

$$\mathbf{F}^{VR}=\begin{bmatrix}0\\ \mu(\nabla\mathbf{v}+\nabla\mathbf{v}^T-\frac{2}{3}(\nabla\cdot\mathbf{v})\mathbf{I})\\ \mu\mathbf{v}^T(\nabla\mathbf{v}+\nabla\mathbf{v}^T-\frac{2}{3}(\nabla\cdot\mathbf{v})\mathbf{I})+\lambda\nabla T+\eta\mathbf{B}^T(\nabla\mathbf{B}-\nabla\mathbf{B}^T)\\ \eta(\nabla\mathbf{B}-\nabla\mathbf{B}^T)\end{bmatrix}$$

Limitations of explicit schemes

Disruption events typically develop **gradually** from near steady-state behaviour in magnetic pressure dominated **low-Mach** number regimes
Would like to use explicit methods for their **shock-capturing** capabilities, but they suffer severe limitations:

- Unfeasible simulation times due to number of time-steps required.
- Inaccurate solutions due to excessive numerical viscocity.

Fast waves not so important for phenomena of interest $\rightarrow$ some form of implicit treatment can help with this

How do we fit in?

Want to design a semi-implicit MHD scheme with the following in mind:

- Solve the equations in conservative form.
- Retain shock-capturing capabilities of fully explicit schemes.
- Treat fast terms implicitly to remove their constraint on the CFL condition (magnetosonic, Alfvén, sound, and diffusive waves).
- Adequately deal with the divergence constraint $\nabla \cdot \mathbf{B} = \mathbf{0}$.

At the base level of the scheme we must find a suitable splitting of the MHD equations, which also has good mathetmatical properties.

Numerical strategy

Motivated by Balsara et al., 2016 we use the following flux splitting:

$$\mathbf{F}^{Conv} = u \begin{bmatrix} \rho \\ \rho u \\ \rho v \\ \rho w \\ \rho k \\ 0 \\ B_y \\ B_z \end{bmatrix}, \quad \mathbf{F}^{PB} = \begin{bmatrix} 0 \\ p + m - B_x^2 \\ -B_x B_y \\ -B_x B_z \\ \rho u h + 2mu - B_x(\mathbf{v} \cdot \mathbf{B}) \\ 0 \\ -v B_x \\ -w B_x \end{bmatrix}$$

- Convective treated **explicitly**, P&B treated **implicitly**.
- Δt is only driven by the eigenvalues of the convective sub-system, in this case just u:

$$\Delta t \leq C_{cfl} \frac{\Delta x}{\max_i |u_i|} .$$

Implicit-explicit discretisation

$$\mathbf{Q}_i^{\star} = \mathbf{Q}_i^n - \frac{\Delta t}{\Delta x}(\hat{\mathbf{F}}^{Conv}_{i+\frac{1}{2}} - \hat{\mathbf{F}}^{Conv}_{i-\frac{1}{2}})$$

- $\mathbf{Q}^{\star}$ is an intermediate state vector.
- The convective sub-system is not strictly hyperbolic. Simple centred Rusanov flux is used for the update formula

$$\hat{\mathbf{F}}^{Conv}_{i+\frac{1}{2}} = \frac{1}{2}(\mathbf{F}^{Conv}(\mathbf{Q}^n_{i+1}) + \mathbf{F}^{Conv}(\mathbf{Q}^n_i)) - \frac{1}{2}S^{max}(\mathbf{Q}^n_{i+1} - \mathbf{Q}^n_i)$$

Implicit subsystem algorithm

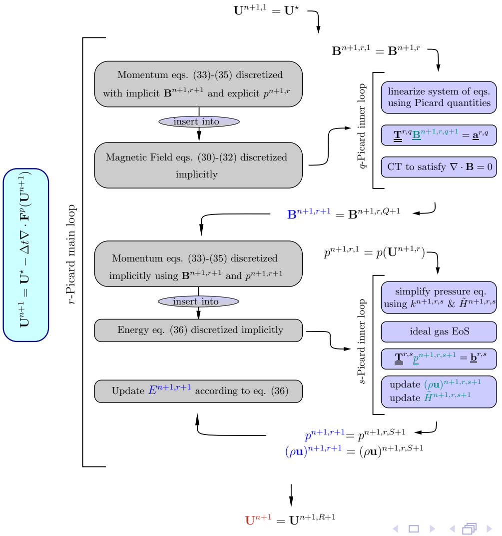

P&B sub-system

Solve a double nested Picard iteration loop:

- Treat non-linear terms as Picard variables
- At each iteration solve a linear system using eg. GMRES

The double nested algorithm:

- Solve implicitly for $\mathbf{B}^{n+1}$ via substitution of $\mathbf{v}$
- Update $\mathbf{v}$ using $\mathbf{B}^{n+1}$ for $\mathbf{v}^{n+1}$
- Solve implicitly for P^{n+1} via substitution of $\mathbf{v}^{n+1}$ and $\mathbf{B}^{n+1}$
- Repeat until convergence

For generic EoS, computation of $(P^{n+1,r+1})$ requires nested Newton

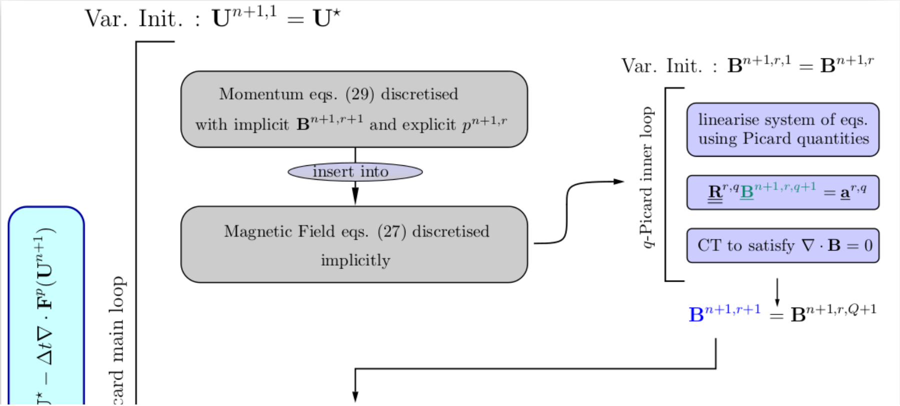
Var. Init. : $\mathbf{U}^{n+1,1} = \mathbf{U}^{\star}$
Momentum eqs. (29) discretised with implicit $\mathbf{B}^{n+1,r+1}$ and explicit $p^{n+1,r}$
insert into
Magnetic Field eqs. (27) discretised implicitly
Var. Init. : $\mathbf{B}^{n+1,r,1} = \mathbf{B}^{n+1,r}$
q-Picard inner loop
linearise system of eqs. using Picard quantities
$\underline{\underline{\mathbf{R}}}^{r,q}\underline{\mathbf{B}}^{n+1,r,q+1} = \underline{\mathbf{a}}^{r,q}$
CT to satisfy $\nabla \cdot \mathbf{B} = 0$
$\mathbf{B}^{n+1,r+1} = \mathbf{B}^{n+1,r,Q+1}$
card main loop
$\mathbf{U}^{\star} - \Delta t \nabla \cdot \mathbf{F}^{p}(\mathbf{U}^{n+1})$

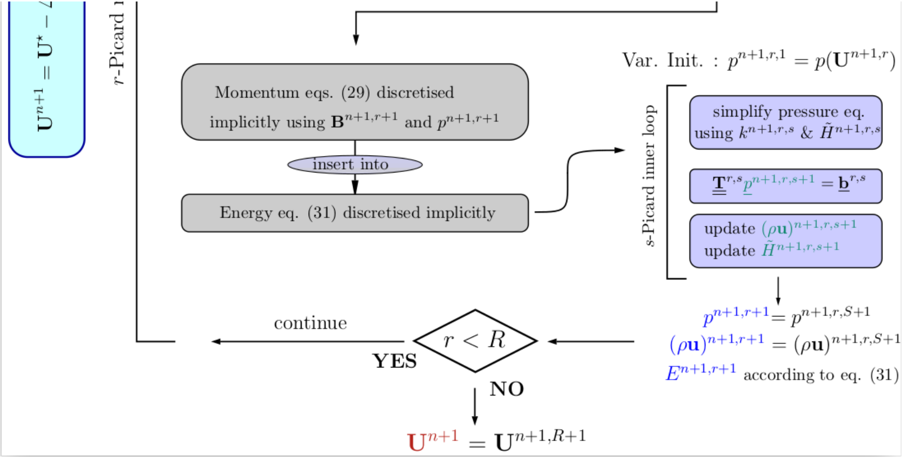
$\mathbf{U}^{n+1} = \mathbf{U}^{\star} -$
r-Picard
Var. Init. : $p^{n+1,r,1} = p(\mathbf{U}^{n+1,r})$
Momentum eqs. (29) discretised implicitly using $\mathbf{B}^{n+1,r+1}$ and $p^{n+1,r+1}$
insert into
Energy eq. (31) discretised implicitly
s-Picard inner loop
simplify pressure eq. using $k^{n+1,r,s}$ & $\tilde{H}^{n+1,r,s}$
$\underline{\underline{\mathbf{T}}}^{r,s}\underline{p}^{n+1,r,s+1} = \underline{\mathbf{b}}^{r,s}$
update $(\rho\mathbf{u})^{n+1,r,s+1}$
update $\tilde{H}^{n+1,r,s+1}$
$p^{n+1,r+1} = p^{n+1,r,S+1}$
$(\rho\mathbf{u})^{n+1,r+1} = (\rho\mathbf{u})^{n+1,r,S+1}$
$E^{n+1,r+1}$ according to eq. (31)
continue
$r < R$
YES
NO
$\mathbf{U}^{n+1} = \mathbf{U}^{n+1,R+1}$

Example equations for $\mathbf{B}^{n+1}$

$$
\begin{cases}
(B_x)_{i,j}^{n+1,r+1} = (B_x)_{i,j}^{\star} + \dfrac{\Delta t}{2\Delta y}\left[(\tilde{b}_y)_{i,j+1/2}^{n+1,r+1}\left((\rho u)_{i,j+1}^{n+1,r+1} + (\rho u)_{i,j}^{n+1,r+1}\right) - (\tilde{b}_y)_{i,j-1/2}^{n+1,r+1}\left((\rho u)_{i,j}^{n+1,r+1} + (\rho u)_{i,j-1}^{n+1,r+1}\right)\right] \\
(B_y)_{i,j}^{n+1,r+1} = (B_y)_{i,j}^{\star} + \dfrac{\Delta t}{2\Delta x}\left[(\tilde{b}_x)_{i+1/2,j}^{n+1,r+1}\left((\rho v)_{i+1,j}^{n+1,r+1} + (\rho v)_{i,j}^{n+1,r+1}\right) - (\tilde{b}_x)_{i-1/2,j}^{n+1,r+1}\left((\rho v)_{i,j}^{n+1,r+1} + (\rho v)_{i-1,j}^{n+1,r+1}\right)\right] \\
(B_z)_{i,j}^{n+1,r+1} = (B_z)_{i,j}^{\star} + \dfrac{\Delta t}{2\Delta x}\left[(\tilde{b}_x)_{i+1/2,j}^{n+1,r+1}\left((\rho w)_{i+1,j}^{n+1,r+1} + (\rho w)_{i,j}^{n+1,r+1}\right) - (\tilde{b}_x)_{i-1/2,j}^{n+1,r+1}\left((\rho w)_{i,j}^{n+1,r+1} + (\rho w)_{i-1,j}^{n+1,r+1}\right)\right] \\
\qquad + \dfrac{\Delta t}{2\Delta y}\left[(\tilde{b}_y)_{i,j+1/2}^{n+1,r+1}\left((\rho w)_{i,j+1}^{n+1,r+1} + (\rho w)_{i,j}^{n+1,r+1}\right) - (\tilde{b}_y)_{i,j-1/2}^{n+1,r+1}\left((\rho w)_{i,j}^{n+1,r+1} + (\rho w)_{i,j-1}^{n+1,r+1}\right)\right]
\end{cases}
$$

with $(\tilde{b}_x)_{i+1/2,j}^{n+1,r+1}$ and $(\tilde{b}_y)_{i,j+1/2}^{n+1,r+1}$ defined as :

$$
\begin{cases}
(\tilde{b}_x)_{i+1/2,j}^{n+1,r+1} = \dfrac{(B_x)_{i,j}^{n+1,r+1} u_{i,j}^{n+1,r+1} + (B_x)_{i+1,j}^{n+1,r+1} u_{i+1,j}^{n+1,r+1}}{(\rho u)_{i,j}^{n+1,r+1} + (\rho u)_{i+1,j}^{n+1,r+1}} \\
(\tilde{b}_y)_{i,j+1/2}^{n+1,r+1} = \dfrac{(B_y)_{i,j}^{n+1,r+1} v_{i,j}^{n+1,r+1} + (B_y)_{i,j+1}^{n+1,r+1} v_{i,j+1}^{n+1,r+1}}{(\rho v)_{i,j}^{n+1,r+1} + (\rho v)_{i,j+1}^{n+1,r+1}}
\end{cases}.
$$

- analogous expressions when solving for the pressure.

Preserving the divergence constraint

- **B** is evolved using discrete version of Faraday induction equation:

$$(B_x)^{n+1}_{i+1/2,j} = (B_x)^n_{i+1/2,j} + \frac{\Delta t}{\Delta y}\left((E_z)^{n+1/2}_{i+1/2,j+1/2} - (E_z)^{n+1/2}_{i+1/2,j-1/2}\right)$$
$$(B_y)^{n+1}_{i,j+1/2} = (B_y)^n_{i,j+1/2} - \frac{\Delta t}{\Delta x}\left((E_z)^{n+1/2}_{i+1/2,j+1/2} - (E_z)^{n+1/2}_{i-1/2,j+1/2}\right)$$

  where $(E_z)^{n+1/2}_{i+1/2,j+1/2}$ is the integral average over Δt of the z-component of the electric field at the grid cell edge $(i+1/2, j+1/2)$.

- It can be easly verified that the discrete divergence condition is satisfied at time t^{n+1} if it was so at time t^n.

Constrained transport for semi-implicit schemes

- We modify the CT algorithm by Gardiner and Stone, where E_z is computed using the four neighbouring face-centred electric field components along with estimates of the gradients, namely

$$
\begin{aligned}
&(E_z)^{n+1/2}_{i+1/2,j+1/2} = (\bar{E}_z)^{n+1/2}_{i+1/2,j+1/2} + \\
&\frac{\Delta x}{8}\left[\left(\frac{\partial E_z}{\partial x}\right)_{i+1/4,j+1/2} - \left(\frac{\partial E_z}{\partial x}\right)_{i+3/4,j+1/2}\right] + \\
&\frac{\Delta y}{8}\left[\left(\frac{\partial E_z}{\partial y}\right)_{i+1/2,j+1/4} - \left(\frac{\partial E_z}{\partial y}\right)_{i+1/2,j+3/4}\right],
\end{aligned}
$$

Constrained transport for semi-implicit schemes

- Compute the first term on the cell edge as average of face fields

$$(\bar{E}_z)^{n+1/2}_{i+1/2,j+1/2} = \frac{1}{4}\Big[(E_z)_{i+1/2,j} + (E_z)_{i+1/2,j+1} + (E_z)_{i,j+1/2} + (E_z)_{i+1,j+$$

- Exploit the dualism between **E** and Godunov fluxes for **B**

$$(E_z)_{i+1/2,j} = -(F_{[B_y]})^a_{i+1/2,j} - (F_{[B_y]})^p_{i+1/2,j} \ ,$$

$$(E_z)_{i,j+1/2} = +(G_{[B_x]})^a_{i,j+1/2} + (G_{[B_x]})^p_{i,j+1/2} \ ,$$

- Electric field derivatives computed according to

$$\left(\frac{\partial E_z}{\partial x}\right)_{i+1/4,j+1/2} = \frac{1}{2}\Big[\frac{(E_z)_{i+1/2,j} - \tilde{E}_{z i,j}}{\Delta x/2} + \frac{(E_z)_{i+1/2,j+1} - \tilde{E}_{z i,j+1}}{\Delta x/2}\Big] \ ,$$

Extension to visco-resistive MHD

- The VR tensor can be re-written in the following form (2D)

$$\nabla \cdot \mathbf{F}^{VR} = \begin{bmatrix} 0 \\ (\tau_{xx})_x + (\tau_{yx})_y \\ (\tau_{xy})_x + (\tau_{yy})_y \\ (\tau_{xz})_x + (\tau_{yz})_y \\ \lambda(\frac{\partial^2 T}{\partial x^2} + \frac{\partial^2 T}{\partial y^2}) + (\Phi_x)_x + (\Phi_y)_y + (\Pi_x)_x + (\Pi_y)_y \\ (R_{xx})_x + (R_{yx})_y \\ (R_{xy})_x + (R_{yy})_y \\ (R_{xz})_x + (R_{yz})_y \end{bmatrix},$$

- Discretise the VR tensor implicitly - using an appropriate local spatial operator get extra terms for the linear system.

Example equations for $\mathbf{B}^{n+1}$

$$
\begin{cases}
(B_x)_{i,j}^{n+1,r+1} = RHS^{ideal}_{[(\tilde{B}_x)_{i,j}^{n+1,r+1}]} \\
\qquad + \dfrac{\Delta t}{\Delta y}\left((R_{yx})_{i,j+1/2}^{n+1,r+1} - (R_{yx})_{i,j-1/2}^{n+1,r+1}\right) , \\
(B_y)_{i,j}^{n+1,r+1} = RHS^{ideal}_{[(\tilde{B}_y)_{i,j}^{n+1,r+1}]} \\
\qquad + \dfrac{\Delta t}{\Delta x}\left((R_{xy})_{i+1/2,j}^{n+1,r+1} - (R_{xy})_{i-1/2,j}^{n+1,r+1}\right) , \\
(B_z)_{i,j}^{n+1,r+1} = RHS^{ideal}_{[(\tilde{B}_z)_{i,j}^{n+1,r+1}]} \\
\qquad + \dfrac{\Delta t}{\Delta x}\left((R_{xz})_{i+1/2,j}^{n+1,r+1} - (R_{xz})_{i-1/2,j}^{n+1,r+1}\right) \\
\qquad + \dfrac{\Delta t}{\Delta y}\left((R_{yz})_{i,j+1/2}^{n+1,r+1} - (R_{yz})_{i,j-1/2}^{n+1,r+1}\right) .
\end{cases}
$$

- Discretisation analogously applied to viscous terms for $\mathbf{v}$ and p.

Numerical Solutions

High Mach number

- Benchmark 1D Riemann problems for the ideal MHD equations

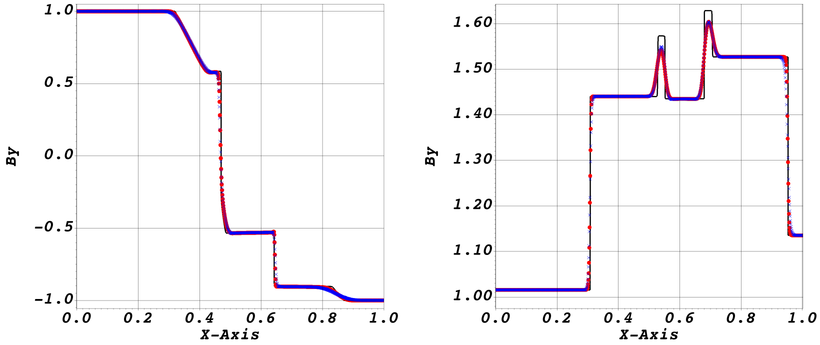

Solution for B_y for RP1 and RP2.

High Mach number

- Orszag-Tang problem, test shock-capturing and transition to supersonic turbulence capabilities of scheme.

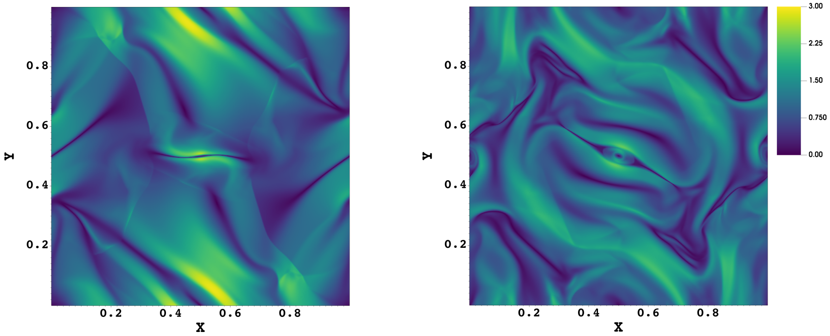

Solution for ρ at time 0.5 (left), time 1.0 (right).

High Mach number

- MHD-Rotor problem, test shock-capturing and ability to handle divergence constraint.

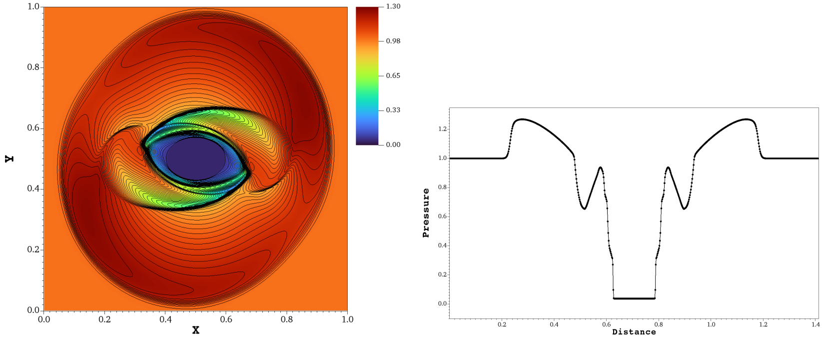

Solution for p at time $t = 0.25$ (left), with 1D cross section (right).

Low Mach number

- Advected θ pinch equilibrium problem, compare performance to explicit schemes.

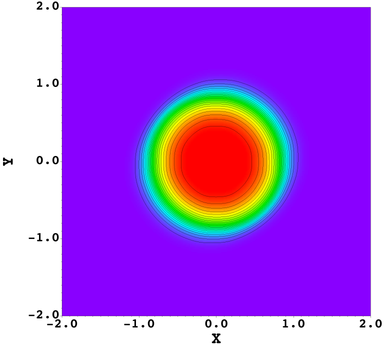

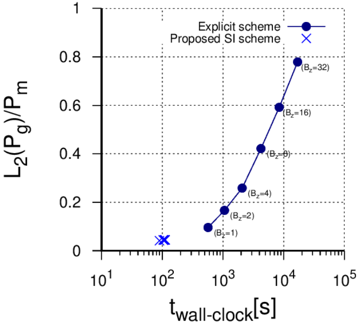

Solution for p at time 100 (left), comparison between semi-implicit and fully explicit scheme (right).

Low Mach number

- Current sheet and Visco-resistive Kelvin-Helmholtz test, test performance for VRMHD equations.

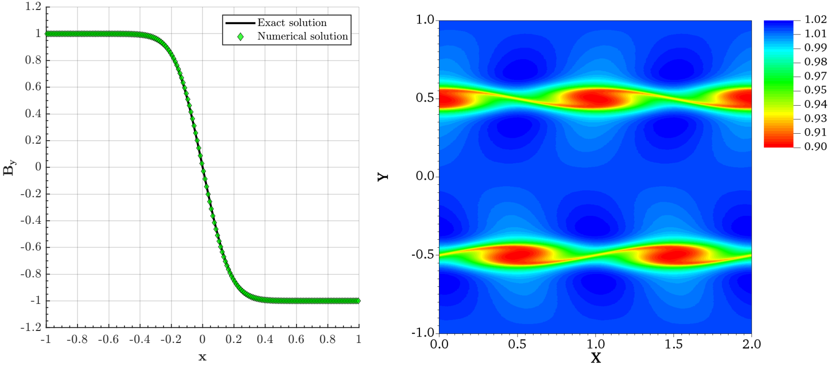

Solution for B_y at time $t = 1.0$ (left) for the current sheet, solution for ρ (right) for VR Kelvin-Helmholtz.

Low Mach number

- Lid-driven cavity with imposed **B**, assess complex BC and incompressible regime.

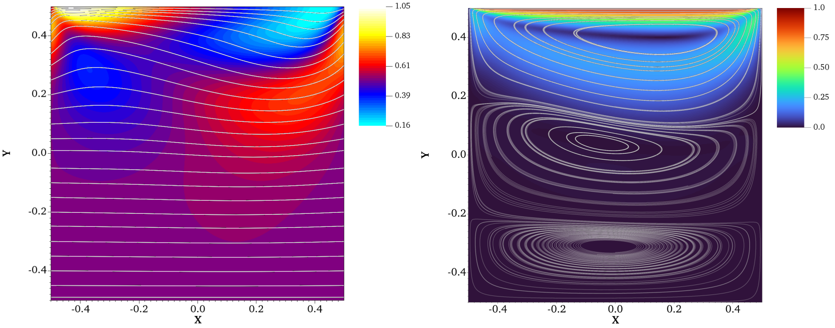

Solution for p_{gas} at time 100 (left), comparison between semi-implicit and fully explicit scheme (right).

- Note - can use a different EoS to simulate e.g. liquid Lithium.

All Mach number

- Plasma washing machine, accelerating lid-velocity with imposed **B**.

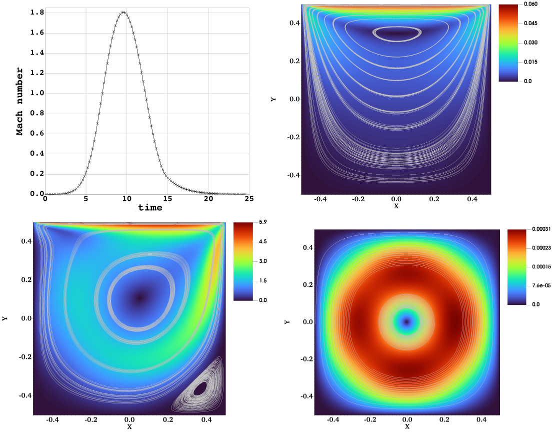

Lid velocity profile (top-left). Solution for u_x at times $t = 3.2, t = 10.0, t = 20.0$.

Plasma washing machine

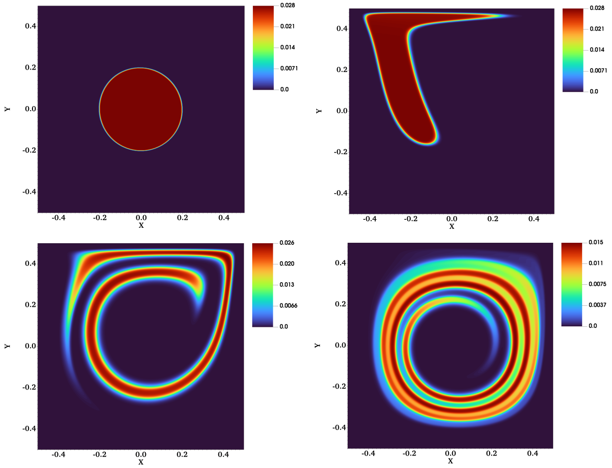

Solution for B_z at times $t = 0.0$, $t = 3.2$,$t = 10.0$,$t = 20.0$.

Conclusions and Future work

- Conlusions
  - Found a suitable splitting of the MHD equations with good mathematical properties.
  - Fast terms are treated implicitly hence CFL condition constrained only by fluid velocity.
  - Scheme validated for low, high, and all Mach number fluid regimes.
- Future work
  - Implementation and validation of rigid-body interaction within semi-implicit scheme.
  - Extension to high order in space and time.
  - Extension of equations (2-fluid) to include more physics.
  - More complex EoS.
  - Simulation of ELMs (Edge Localised Modes)!

Thank you for listening!

Supplementary slides follow

Divergence error

- Divergence error remains to machine precision levels:

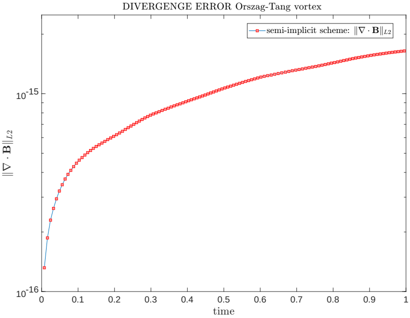

Solution for $\nabla \cdot \mathbf{B}$ throughout Orszag-Tang test.

High-Mach

- Benchmark 1D Riemann problems for the ideal MHD equations

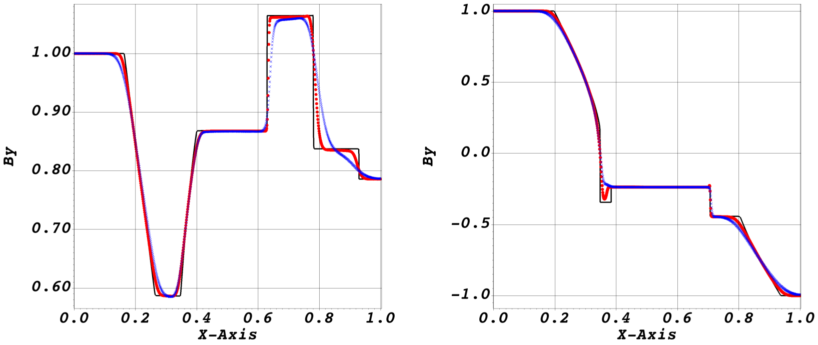

Solution for B_y for RP3 and RP4.

Low-Mach

- Advected screw-pinch equilibrium, test low-Mach behaviour of scheme.

$$\rho = 1.0, \;\; \mathbf{v} = (2.0, 2.0, 0.0)\,,$$

$$\mathbf{B} = \begin{cases} (0.0, 0.0, B_0 \dfrac{r^2}{R^2}), & \text{if } 0 \le r \le R \\ (0.0, 0.0, B_0) & \text{otherwise} \end{cases}$$

$$p = \begin{cases} \dfrac{1}{2}(B_0^2 - B_z^2) + 0.1, & \text{if } 0 \le r \le R \\ 0.1 & \text{otherwise} \end{cases}$$

Validating all-mach capabilities of scheme

- In tokamaks, fluid behaviour ranges from very low to high mach number during course of operation.
- So far, none such tests demonstrated in literature.
- Inspired by lid-driven cavity test devise such a test using an accelerating top boundary for changing Mach number of flow.

$$u_{lid} = u_{max} e^{\frac{(t - t_{peak})^2}{2\sigma}} \tag{1.1}$$

- Initialise circular region of constant $Bz = 0.1$ to be advected by the flow.
- The result is an MHD test problem exhibiting both low and high mach regimes of flow.

Accelerating lid-driven cavity

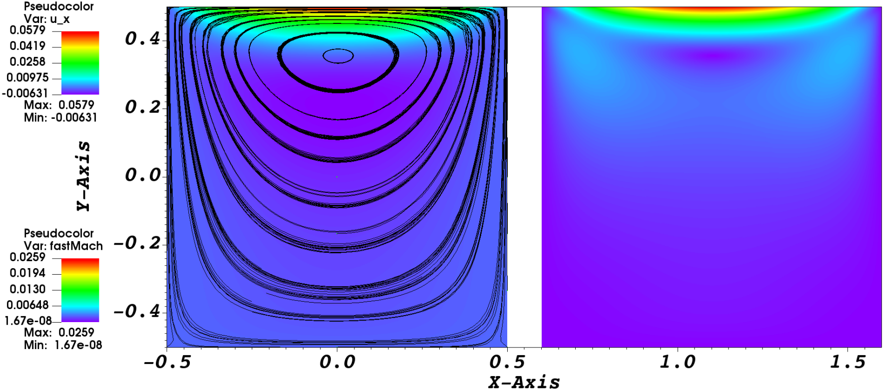

Solution for u (left), Mach number (right) at t = 3.2.

Accelerating lid-driven cavity

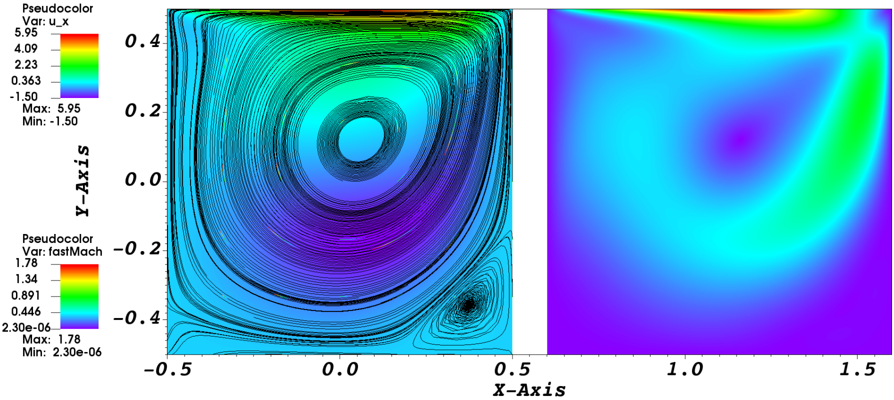

Solution for u (left), Mach number (right) at t = 10.0.

Accelerating lid-driven cavity

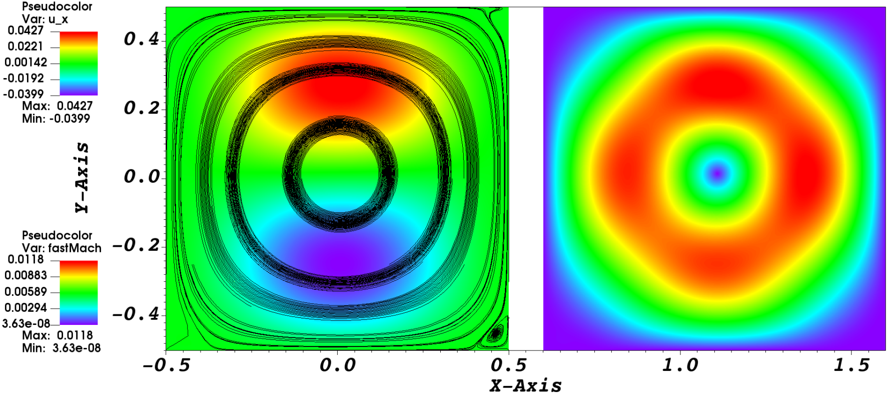

Solution for u (left), Mach number (right) at t = 20.0.

Accelerating lid-driven cavity

Start Video

Inclusion of multi-material interface

- Using rigid-body GFM to assign BC for the fluid

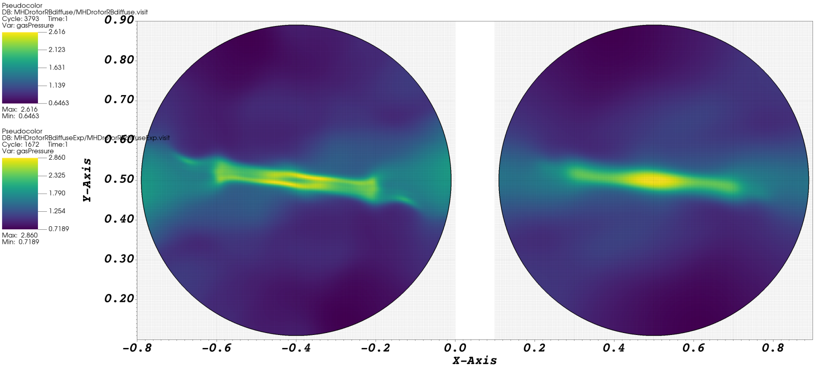

MHD rotor inside rigid circle, comparing P&B to explicit.

Divergence cleaning

$\mathbf{B}^\star$ obtained by the base scheme projected onto the subspace of zero divergence solutions (Helmholtz decomposition):

$$\mathbf{B}^\star = \nabla \times \mathbf{A} + \nabla\phi \tag{1.2}$$

$$\nabla^2\phi = \nabla\cdot\mathbf{B}^\star \tag{1.3}$$

$$\mathbf{B}^{n+1} = \mathbf{B}^\star - \nabla\phi \tag{1.4}$$

- Solve Poisson equation (1.7) for ϕ.

$$\frac{\phi_{i-2,j,k} - 2\phi_{i,j,k} + \phi_{i+2,j,k}}{4(\Delta x)^2} + \frac{\phi_{i,j-2,k} - 2\phi_{i,j,k} + \phi_{i,j+2,k}}{4(\Delta y)^2} = \frac{Bx^\star_{i+1,j,k} - Bx^\star_{i-1,j,k}}{2\Delta x} + \frac{By^\star_{i,j+1,k} - By^\star_{i,j-1,k}}{2\Delta y} \tag{1.5}$$

Divergence cleaning

$\mathbf{B}^\star$ obtained by the base scheme projected onto the subspace of zero divergence solutions (Helmholtz decomposition):

$$\mathbf{B}^\star = \nabla \times \mathbf{A} + \nabla\phi \tag{1.6}$$

$$\nabla^2\phi = \nabla \cdot \mathbf{B}^\star \tag{1.7}$$

$$\mathbf{B}^{n+1} = \mathbf{B}^\star - \nabla\phi \tag{1.8}$$

- Solve Poisson equation (1.7) for ϕ.

$$\frac{\phi_{i-2,j,k} - 2\phi_{i,j,k} + \phi_{i+2,j,k}}{4(\Delta x)^2} + \frac{\phi_{i,j-2,k} - 2\phi_{i,j,k} + \phi_{i,j+2,k}}{4(\Delta y)^2} = \frac{Bx^\star_{i+1,j,k} - Bx^\star_{i-1,j,k}}{2\Delta x} + \frac{By^\star_{i,j+1,k} - By^\star_{i,j-1,k}}{2\Delta y} \tag{1.9}$$

Scalar Divergence Cleaning

- It is based on solving the Poisson equation (1.7) for ϕ. This can be done either in physical space

$$\frac{\phi_{i-2,j,k} - 2\phi_{i,j,k} + \phi_{i+2,j,k}}{4(\Delta x)^2} + \frac{\phi_{i,j-2,k} - 2\phi_{i,j,k} + \phi_{i,j+2,k}}{4(\Delta y)^2} = \frac{Bx^{\star}_{i+1,j,k} - Bx^{\star}_{i-1,j,k}}{2\Delta x} + \frac{By^{\star}_{i,j+1,k} - By^{\star}_{i,j-1,k}}{2\Delta y} \qquad (1.10)$$

  or in Fourier space after having computed the Fourier transform of $\nabla \cdot \mathbf{B}^{\star}$

- if the Poisson equation for ϕ is solved in the Fourier space and the domain is not periodic one can use an even/odd extension to apply Dirichlet/Neumann boundary conditions.

Scalar Divergence Cleaning

- To avoid odd-even decoupling, Balsara recommends a different discritisation - though this does not "clean" as effectively, due to an inconsistent discritisation.

$$\frac{\phi_{i-1,j,k} - 2\phi_{i,j,k} + \phi_{i+1,j,k}}{(\Delta x)^2} + \frac{\phi_{i,j-1,k} - 2\phi_{i,j,k} + \phi_{i,j+1,k}}{(\Delta y)^2} = \frac{Bx^{\star}_{i+1,j,k} - Bx^{\star}_{i-1,j,k}}{2\Delta x} + \frac{By^{\star}_{i,j+1,k} - By^{\star}_{i,j-1,k}}{2\Delta y} \quad (1.11)$$

P & B implicit: 3-split scheme

- The implicitly treated system is further split into two systems, resulting in the 3-split formulation:

$$\mathbf{F}^{Conv} = u \begin{bmatrix} \rho \\ \rho u \\ \rho v \\ \rho w \\ \rho k \\ 0 \\ B_y \\ B_z \end{bmatrix}, \quad \mathbf{F}^{Pres} = \begin{bmatrix} 0 \\ p \\ 0 \\ 0 \\ \rho u h \\ 0 \\ 0 \\ 0 \end{bmatrix}, \quad \mathbf{F}^{B} = \begin{bmatrix} 0 \\ m - B_x^2 \\ -B_x B_y \\ -B_x B_z \\ 2mu - B_x(\mathbf{v} \cdot \mathbf{B}) \\ 0 \\ -vB_x \\ -wB_x \end{bmatrix} \qquad (1.12)$$

Convective sub-system

$$\mathbf{Q}_i^\star = \mathbf{Q}_i^n - \frac{\Delta t}{\Delta x}(\hat{\mathbf{F}}^{Conv}_{i+\frac{1}{2}} - \hat{\mathbf{F}}^{Conv}_{i-\frac{1}{2}}) \tag{1.13}$$

- $\mathbf{Q}^\star$ is an intermediate state vector.
- The convective sub-system is not strictly hyperbolic. Simple centred Rusanov flux is used for the update formula

$$\hat{\mathbf{F}}^{Conv}_{i+\frac{1}{2}} = \frac{1}{2}(\mathbf{F}^{Conv}(\mathbf{Q}^n_{i+1}) + \mathbf{F}^{Conv}(\mathbf{Q}^n_i)) - \frac{1}{2}S^{max}(\mathbf{Q}^n_{i+1} - \mathbf{Q}^n_i) \tag{1.14}$$

- The choice of Δt is only driven by the eigenvalues of the convective sub-system:

$$\Delta t \leq C_{cfl}\frac{\Delta x}{\max_i |u_i|} \ . \tag{1.15}$$

First order implicit-explicit discretisation

Pressure sub-system

- it involves only the momentum and the the total energy equations.

$$\epsilon^2 \Delta x (\rho e)_i^{n+1} - \frac{\Delta t^2}{\Delta x}\left(-(\frac{3}{4}\tilde{h}_{i-1} + \frac{1}{4}\tilde{h}_{i+1})p_{i-1}^{n+1} + (\tilde{h}_{i-1} + \tilde{h}_{i+1})p_i^{n+1} + (\frac{1}{4}\tilde{h}_{i-1}^{n+1,r+1} + \frac{3}{4}\tilde{h}_{i+1}^{n+1,r+1})p_{i+1}^{n+1}\right)$$
$$= \epsilon^2 \Delta x \left(E_i^\star - \tilde{k}_i^{n+1,r+1} - \frac{\Delta t}{2\Delta x}\left(\tilde{h}_{i+1}^{n+1,r+1}(\rho u)_{i+1}^\star - \tilde{h}_{i-1}^{n+1,r+1}(\rho u)_{i-1}^\star\right)\right)$$

  where the tilde terms $\tilde{()}_i^{n+1,r+1}$ denote simple Picard iterations
- In compact form:

$$\underline{\mathcal{E}}^{nl}(\underline{P}^{n+1,r+1}) + \underline{\underline{\mathcal{R}}} \cdot \underline{P}^{n+1,r+1} = \underline{b} \qquad (1.13)$$

- For an ideal gas the term $\underline{\mathcal{E}}^{nl}(\underline{P}^{n+1,r+1})$ is linear
- For a generic EoS, the computation of the pressures $(\underline{P}^{n+1,r+1})$ requires the use of a Nested Newton method

Multi-material simulation

- MHD rotor problem placed inside rigid container.
- Initial discontinuity in density and angular velocity profile.
- Evolution of gas pressure with time:

Start Video

1D Validation and comparison

- RP test no. 1

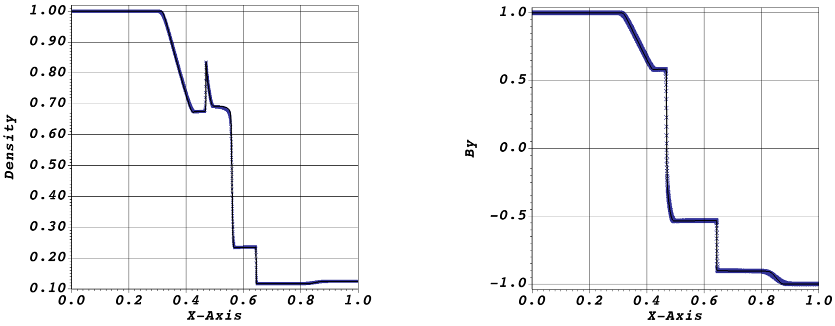

Semi-implicit solution (points, 4000 cells) plotted over explicit reference solution (line, 10000 cells)

1D Validation and comparison

- RP test no. 2

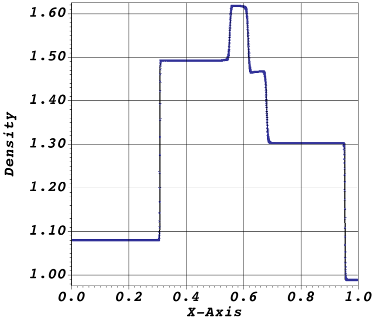

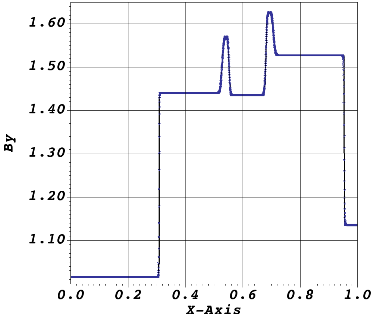

Semi-implicit solution (points, 4000 cells) plotted over explicit reference solution (line, 10000 cells)

1D Validation and comparison

- RP test no. 3

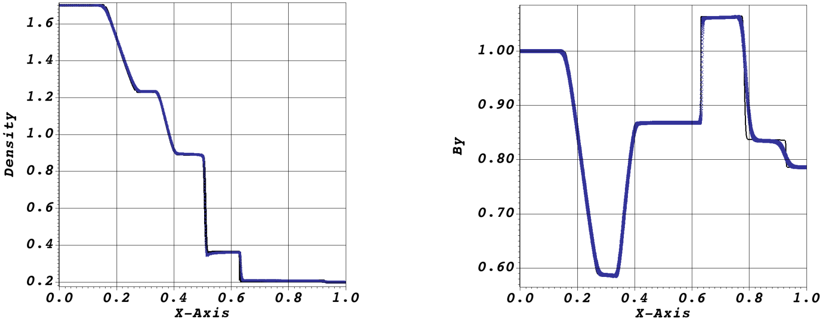

Semi-implicit solution (points, 4000 cells) plotted over explicit reference solution (line, 10000 cells)

1D Validation and comparison

- RP test no. 3 with Alfvenic timestep

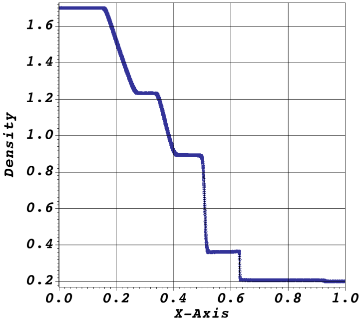

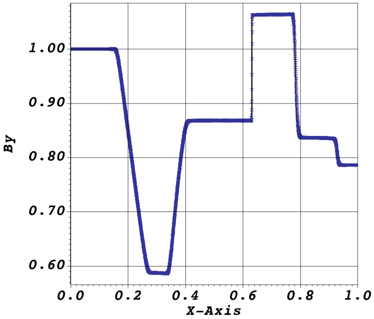

Semi-implicit solution (points, 4000 cells) plotted over explicit reference solution (line, 10000 cells)

1D Validation and comparison

- RP test no. 4

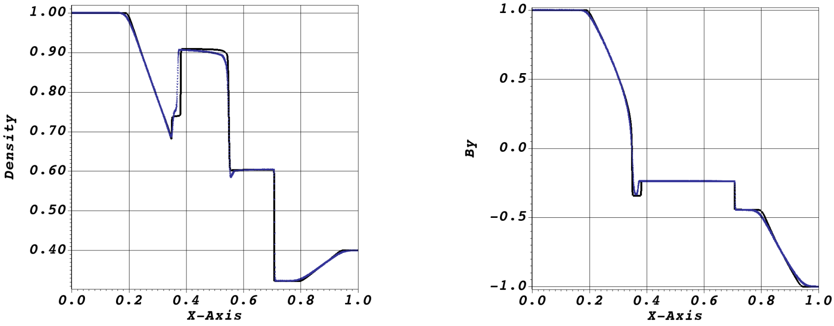

Semi-implicit solution (points, 4000 cells) plotted over explicit reference solution (line, 10000 cells)

3-Split - Low Mach

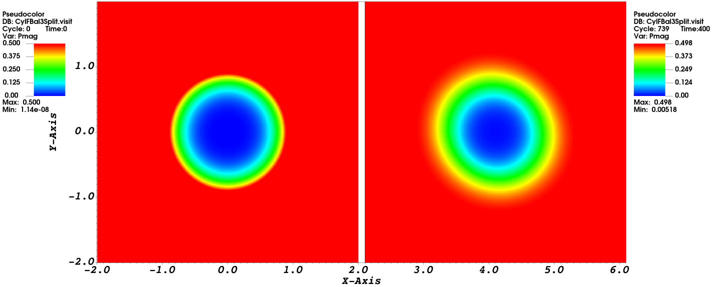

Solution for total pressure at t = 0 (left) and t = 400.0 (right) for P&B.

Validation for resistivity..

- Consider a very challenging version of current sheet test :
- $\eta = 0.1$, $|B_y| = 1e-3$, $B_z = 1e4$, $p = 1e5$, CFL $= 1000$

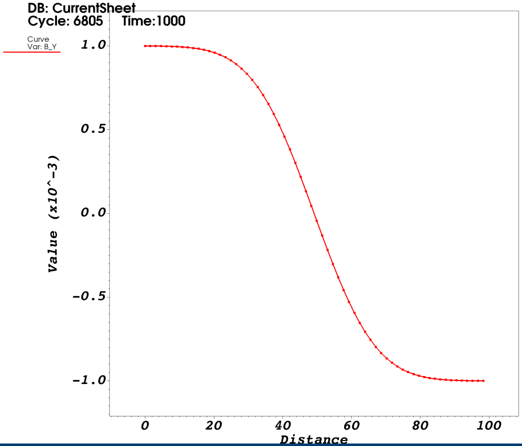

2D tests

- Harris-Reconnection with $\eta = 0.01$

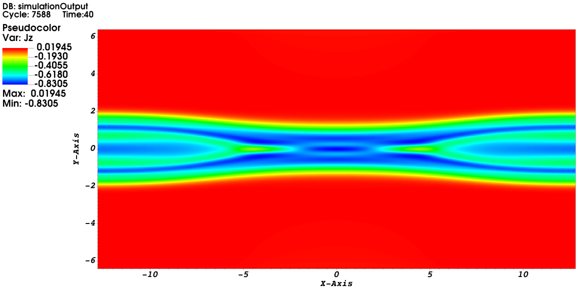

Viscocity implicit - 1D

- Fully implicit viscous terms now working in 1D for shear layer test:

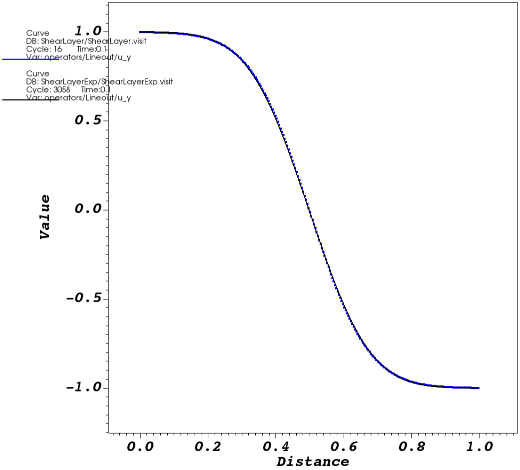

Heat flux implicit

- To treat heat flux implicitly must express temperature as a function of pressure to be inserted into pressure subsystem.
- Contribution to pressure sub-system if the laplacian of this.
- For ideal-gas EoS this is relatively straightforward:

$$T = \frac{1}{c_v} \frac{p}{(\gamma - 1)\rho} \tag{1.14}$$

$$\frac{\partial^2 T}{\partial x^2} = \frac{\frac{\partial^2 p}{\partial x^2}}{c_v \rho (\gamma - 1)} - \frac{2\frac{\partial p}{\partial x}\frac{\partial \rho}{\partial x}}{c_v \rho^2 (\gamma - 1)} + \frac{2p(\frac{\partial \rho}{\partial x})^2}{c_v \rho^3 (\gamma - 1)} - \frac{p\frac{\partial^2 \rho}{\partial x^2}}{c_v \rho^2 (\gamma - 1)} \tag{1.15}$$

- These terms must then be inserted into the equation for pressure.

Heat flux implicit

- Heat flux test taken from Boscheri - discontinuity in density causes heat transfer.

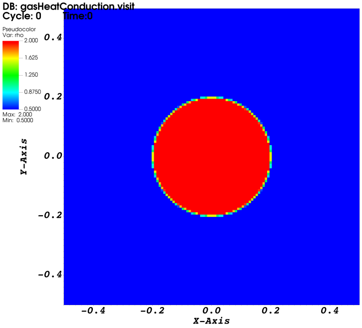

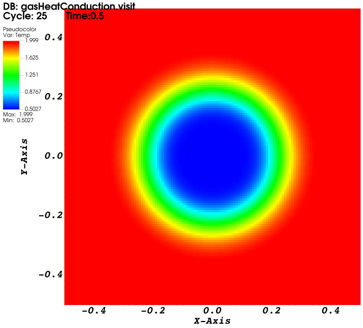

Heat flux implicit

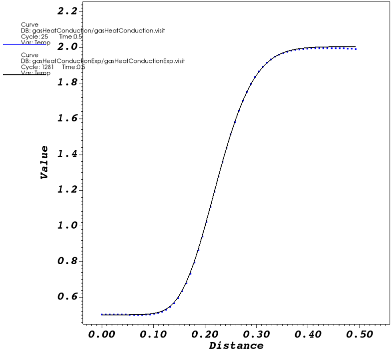

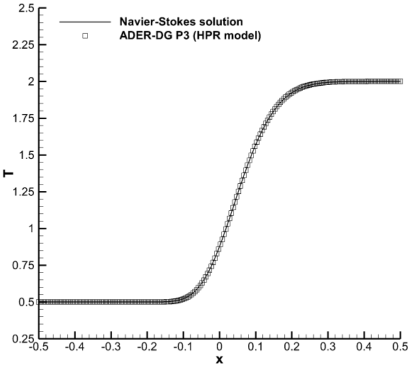

Viscocity and heat-flux implicit, high order extension

- Testing the robustness of all components working together.
- Double shear-layer test, requires very high accuracy to see the fine features, Re $= 5000$.
- Horizontal Jets with slight velocity perturbation - two shear-layers which roll up over time.

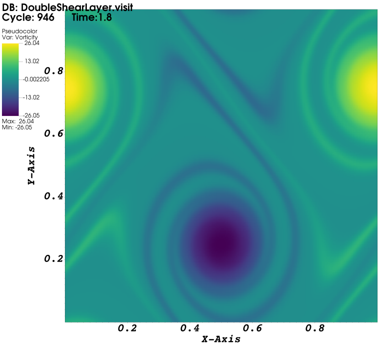

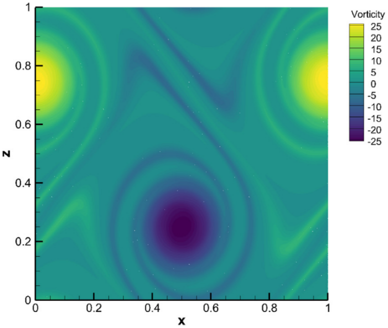

Kelvin-Helmholtz VRMHD

- KH-VRMHD with viscocity,resistivity and heat flux treated implicitly.

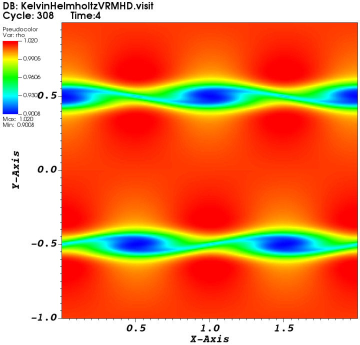

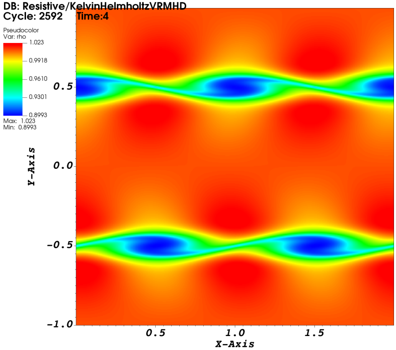

A challenging problem - lid-driven cavity test, M=0.1

- Constant ρ, p, and zero flow everywhere.
- No-slip BC apart from parabolic velocity on top boundary for u_x.
- Equivalent CFL of 100 compared to explicit viscocity.
- Note: different IC than ref - they use constant u for the lid.

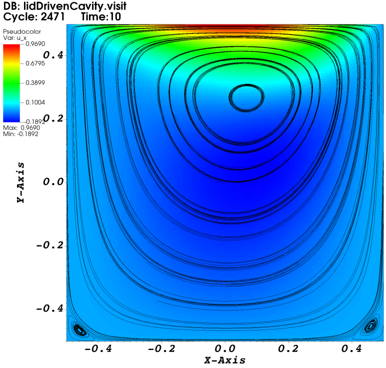

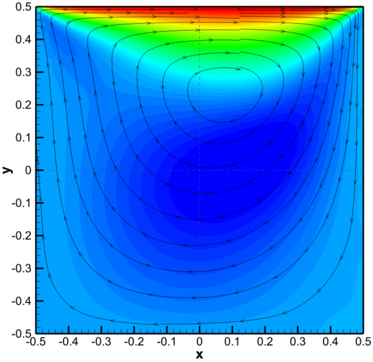

All-mach lid-driven cavity.. Eulers washing machine..

- Begin with lid velocity of zero and ramp up to exponentially increase in time.
- Stop at some maximum velocity.

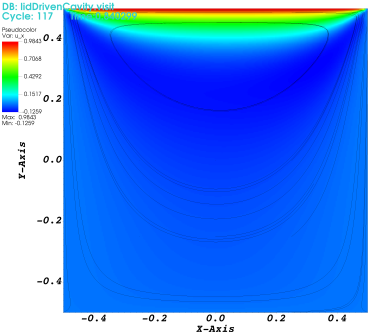

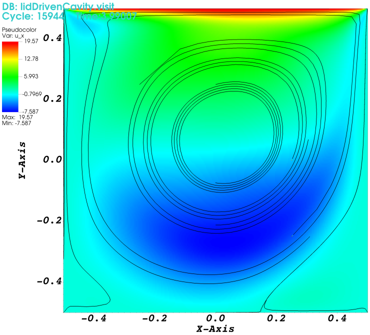

All-mach lid-driven cavity.. Eulers washing machine..